

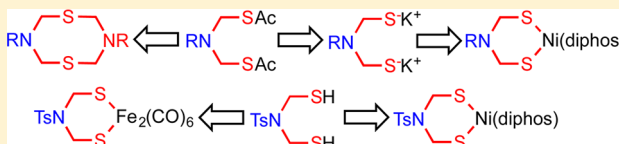
N-Substituted Derivatives of the Azadithiolate Cofactor from the [FeFe] Hydrogenases: Stability and Complexation

Raja Angamuthu,[†] Chi-Shian Chen, Tyler R. Cochrane, Danielle L. Gray, David Schilter, Olbelina A. Ulloa, and Thomas B. Rauchfuss*

School of Chemical Sciences, University of Illinois at Urbana–Champaign, Urbana, Illinois 61801, United States

Supporting Information

ABSTRACT: Experiments are described that probe the stability of N-substituted derivatives of the azadithiolate cofactor recently confirmed in the [FeFe] hydrogenases (Berggren, G., et al. *Nature* **2013**, 499, 66). Acid-catalyzed hydrolysis of bis(thioester) $\text{BnN}(\text{CH}_2\text{SAc})_2$ gives $[\text{BnNCH}_2\text{SCH}_2]_2$ rather than azadithiol $\text{BnN}(\text{CH}_2\text{SH})_2$. Treatment of $\text{BnN}(\text{CH}_2\text{SAc})_2$ with NaO^tBu generates $\text{BnN}(\text{CH}_2\text{SNa})_2$, which was trapped with $\text{NiCl}_2(\text{diphos})$ (diphos = 1,2- $\text{C}_2\text{H}_4(\text{PR}_2)_2$; R = Ph (dppe) and Cy (dcpe)) to give fully characterized complexes $\text{Ni}[(\text{SCH}_2)_2\text{NBn}](\text{diphos})$. The related N-aryl derivative $\text{Ni}[(\text{SCH}_2)_2\text{NC}_6\text{H}_4\text{Cl}](\text{diphos})$ was prepared analogously from 4- $\text{ClC}_6\text{H}_4\text{N}(\text{CH}_2\text{SAc})_2$, NaO^tBu , and $\text{NiCl}_2(\text{dppe})$. Crystallographic analysis confirmed that these rare nonbridging $[\text{adt}^{\text{R}}]^{2-}$ complexes feature distorted square planar Ni centers. The analogue $\text{Pd}[(\text{SCH}_2)_2\text{NBn}](\text{dppe})$ was also prepared. ^{31}P NMR analysis indicates that $\text{Ni}[(\text{SCH}_2)_2\text{NBn}](\text{dppe})$ has basicity comparable to typical amines. As shown by cyclic voltammetry, the couple $[\text{M}[(\text{SCH}_2)_2\text{NBn}](\text{dppe})]^{+/0}$ is reversible near -2.0 V versus $\text{Fc}^{+/0}$. The wave shifts to -1.78 V upon N-protonation. In the presence of $\text{CF}_3\text{CO}_2\text{H}$, $\text{Ni}[(\text{SCH}_2)_2\text{NBn}](\text{dppe})$ catalyzes hydrogen evolution at rate of 22 s^{-1} in the acid-independent regime, at room temperature in CH_2Cl_2 solution. In contrast to the instability of $\text{RN}(\text{CH}_2\text{SH})_2$ (R = alkyl, aryl), the dithiol of tosylamide $\text{TsN}(\text{CH}_2\text{SH})_2$ proved sufficiently stable to allow full characterization. This dithiol reacts with $\text{Fe}_3(\text{CO})_{12}$ and, in the presence of base, $\text{NiCl}_2(\text{dppe})$ to give $\text{Fe}_2[(\text{SCH}_2)_2\text{NTs}](\text{CO})_6$ and $\text{Ni}[(\text{SCH}_2)_2\text{NTs}](\text{dppe})$, respectively.



INTRODUCTION

The identity of the dithiolate cofactor that supports the activity of the [FeFe] hydrogenases has been actively discussed since the original crystallographic descriptions of the enzymes¹ from *D. desulfuricans* and *C. pasteurianum*. Model studies show that the amine in azadithiolates facilitates protonation of its Fe(I)Fe(I) derivatives (Figure 1).^{2,3} Furthermore, amine-

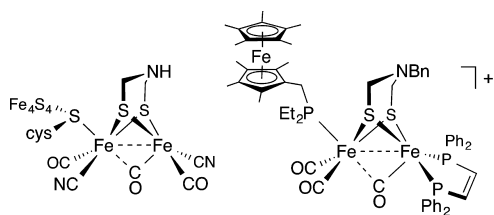


Figure 1. Active site of the H-cluster in [FeFe] hydrogenase enzyme (left) and typical model complex (right).

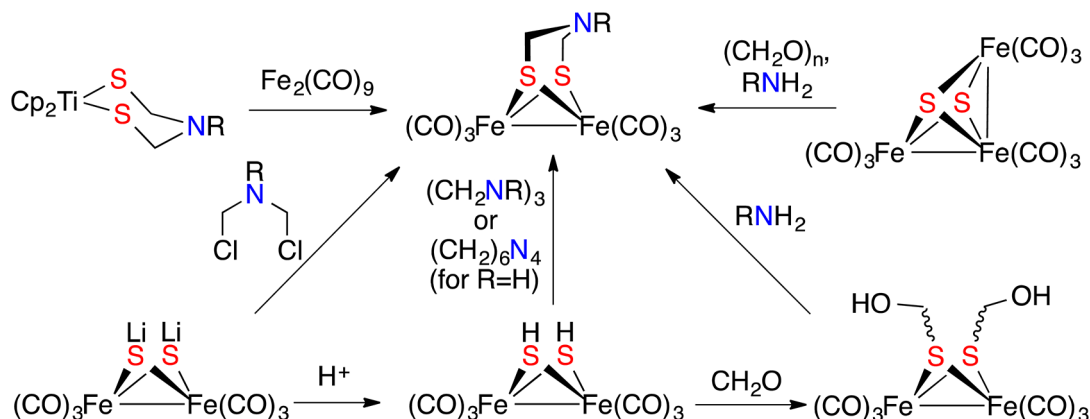
containing dithiolates are required for oxidation of H_2 by mildly electrophilic $\text{Fe}(\text{II})\text{Fe}(\text{I})$ species.⁴ The idea⁵ of an amine poised close but not coordinated to a metal center has spawned the development of homogeneous catalysts featuring proton relays⁶ and is a foundation of our understanding of the second coordination sphere.⁷

The first spectroscopic evidence for the azadithiolate cofactor versus, say, 1,3-propanedithiolate, came from electron–nuclear

double resonance studies on [FeFe] hydrogenases that revealed coupling of Fe(I) to two ^{14}N centers, proposed to be the CN[−] cofactor and the azadithiolate bridge.⁸ This assignment is supported by recent work on the C^{15}N -enriched enzyme.^{9,10} The nature of the dithiolate has finally been settled, with experiments showing that synthetic $[\text{Fe}_2[(\text{SCH}_2)_2\text{NH}](\text{CN})_2(\text{CO})_4]^{2-}$ reconstitutes apo-HydA1 from *C. reinhardtii* to give a highly active catalyst. Isostructural diiron complexes $[\text{Fe}_2(\text{S}_2\text{C}_3\text{H}_6)(\text{CN})_2(\text{CO})_4]^{2-}$ and $[\text{Fe}_2[(\text{SCH}_2)_2\text{O}](\text{CN})_2(\text{CO})_4]^{2-}$ are also accepted by the apoenzyme,^{11,12} but the resulting proteins exhibit very low catalytic activity.¹²

Now that the azadithiolate cofactor has been confirmed, it is of interest to examine the cofactor itself, free of the protein and, if possible, metals. First reported in 2001,¹³ complexes of $[\text{adt}^{\text{R}}]^{2-}$ can be prepared by many routes, almost all of which involve installation of the cofactor on diiron centers (Scheme 1).^{13–16} Typical routes include condensation of CH_2O and amines with $\text{Fe}_2(\text{SH})_2(\text{CO})_6$ ^{14,16} and alkylation of $\text{Fe}_2(\mu\text{-SLi})_2(\text{CO})_6$, the latter route only suited for tertiary amines of the type $\text{RN}(\text{CH}_2\text{Cl})_2$.¹³ Related complexes have been developed with an azadiphosphide group ($\text{RN}(\text{CH}_2\text{PR})_2$)¹⁷ and a azadiselenide ($\text{RN}(\text{CH}_2\text{Se})_2$)¹⁸ bridging two iron centers.

Received: February 6, 2015

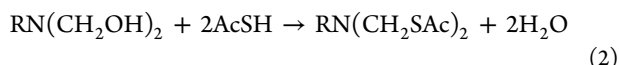
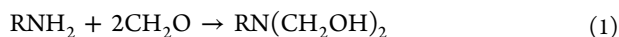
Scheme 1. Synthetic Routes to $\text{Fe}_2[(\text{SCH}_2)_2\text{NR}](\text{CO})_6$ 

In terms of obtaining the *free* cofactor, the diiron dithiolates represent obvious precursors to $\text{RN}(\text{CH}_2\text{SH})_2$. Azadithiolato diiron complexes are, however, robust and exhibit no tendency to release the cofactor even in the presence of strong acids.

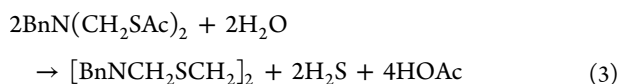
Free $\text{HN}(\text{CH}_2\text{SH})_2$ and related derivatives might be anticipated to be unstable with respect to loss of hydrogen sulfide. This anticipated reactivity necessitates that the azadithiolates or their protonated derivatives be generated under mild reaction conditions. The bis(thioester) compounds of type $\text{RN}(\text{CH}_2\text{SAC})_2$ emerged as attractive precursors to the azadithiolates. Indeed, hydrolysis of one such thioester has been claimed to afford $[\text{HOC}_2\text{H}_4\text{N}(\text{H})(\text{CH}_2\text{SH})_2]\text{Cl}$, the conjugate acid of an azadithiol.¹⁹

RESULTS AND DISCUSSION

Preparation and Hydrolysis of $\text{BnN}(\text{CH}_2\text{SAC})_2$. Hydroxymethylation of primary amines in the presence of thioacetic acid is known to efficiently give bis(thioesters) $\text{RN}(\text{CH}_2\text{SAC})_2$.²⁰ The relevant transformations are given in eqs 1 and 2.



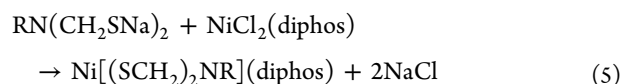
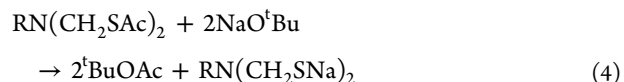
This method appears general, and the initial phases of this study focused on benzyl derivatives. The acid-catalyzed hydrolysis of $\text{BnN}(\text{CH}_2\text{SAC})_2$ was investigated as a route to the dithiol $\text{BnN}(\text{CH}_2\text{SH})_2$. Upon treatment with aqueous HCl in EtOH, $\text{BnN}(\text{CH}_2\text{SAC})_2$ was rapidly consumed with formation of a precipitate. ^1H NMR analysis of the crude product with an internal standard showed that $[\text{BnNCH}_2\text{SCH}_2]_2$ was present in ~60% yield. The reaction does not yield NMR-detectable amounts of trithiane $(\text{SCH}_2)_3$, a result consistent with the stoichiometry in eq 3.



Experiments were conducted testing the utility of $[\text{RNCH}_2\text{SCH}_2]_2$ and the bis(thioesters) as precursors to diiron azadithiolate complexes. Reaction of $[\text{RNCH}_2\text{SCH}_2]_2$ with $\text{Fe}_3(\text{CO})_{12}$ yields $\text{Fe}_2(\text{SCH}_2\text{N}(\text{R})\text{CH}_2)(\text{CO})_6$ instead of the typical $\text{Fe}_2[(\text{SCH}_2)_2\text{NBn}](\text{CO})_6$ derivatives featuring Fe_2S_2 tetrahedranes.²¹ Additionally, reaction of $\text{BnN}(\text{CH}_2\text{SAC})_2$

with $\text{Fe}_3(\text{CO})_{12}$ gave complex mixtures containing only traces of $\text{Fe}_2[(\text{SCH}_2)_2\text{NBn}](\text{CO})_6$.

Trapping $\text{RN}(\text{CH}_2\text{SNa})_2$ ($\text{R} = \text{Bn}$ or $4\text{-ClC}_6\text{H}_4$). Given the instability of azadithiol $\text{RN}(\text{CH}_2\text{SH})_2$ implicated by the previous experiments, the preparation of the corresponding dithiolate dianion was investigated. Treatment of $\text{BnN}(\text{CH}_2\text{SAC})_2$ with NaOMe in MeOH afforded mainly the known diether $\text{BnN}(\text{CH}_2\text{OMe})_2$. A bulkier nucleophile might favor attack at the carbonyl centers instead of the methylene groups, and avoidance of protic solvents would preclude formation of any thiols, these being prone to the degradation pathway in eq 3. Indeed, experiments suggest that the dithiolate can be generated by treatment of $\text{RN}(\text{CH}_2\text{SAC})_2$ ($\text{R} = \text{Bn}$, $4\text{-ClC}_6\text{H}_4$) with NaO^tBu in tetrahydrofuran (THF) at -78°C . The putative $\text{RN}(\text{CH}_2\text{SNa})_2$ was derivatized by treatment with $\text{NiCl}_2(\text{diphos})$ ($\text{diphos} = 1,2\text{-C}_2\text{H}_4(\text{PR}'_2)_2$; $\text{R}' = \text{Ph}$ (dppe) and Cy (dcpe)). These trapping experiments afforded modest yields of orange microcrystalline solids identified as $\text{Ni}[(\text{SCH}_2)_2\text{NR}](\text{diphos})$ (eqs 4 and 5).



In the case of the electrophile $\text{NiCl}_2(\text{dppe})$, the derivative $\text{Ni}[(\text{SCH}_2)_2\text{NR}](\text{dppe})$ was isolated and characterized according to ^1H and $^{31}\text{P}\{^1\text{H}\}$ NMR and electrospray ionization mass spectrometry (ESI-MS) data. The complexes were stable as solids and in THF, CH_2Cl_2 , and MeCN solution under an inert atmosphere. Single crystals of $\text{Ni}[(\text{SCH}_2)_2\text{NR}](\text{dppe})$ were grown from CH_2Cl_2 /pentane. The solid-state structures of the two compounds are presented in Figures 2 and 3.

Crystallographic analysis revealed that $\text{Ni}[(\text{SCH}_2)_2\text{NBn}](\text{dppe})$ features a twisted NiS_2P_2 coordination. The average $\text{Ni}-\text{S}$ (2.185 Å) and $\text{Ni}-\text{P}$ bond lengths (2.176 Å) are similar to those in the propanedithiolate $\text{Ni}(\text{S}_2\text{C}_3\text{H}_6)(\text{dppe})$ (2.203 and 2.160 Å, respectively).²² Substitution, however, of CH_2 with NBn causes distortion of the ligand environment such that the NiS_2 and NiP_2 planes in $\text{Ni}[(\text{SCH}_2)_2\text{NBn}](\text{dppe})$ are twisted by 19.6° (this value being 7.6° for the propane-dithiolate). In the crystal, the Bn group participates in weak edge-to-face $\pi-\pi$ stacking (4.3 Å) with the dppe ligand of a neighboring complex, orienting Bn toward Ni . In addition to

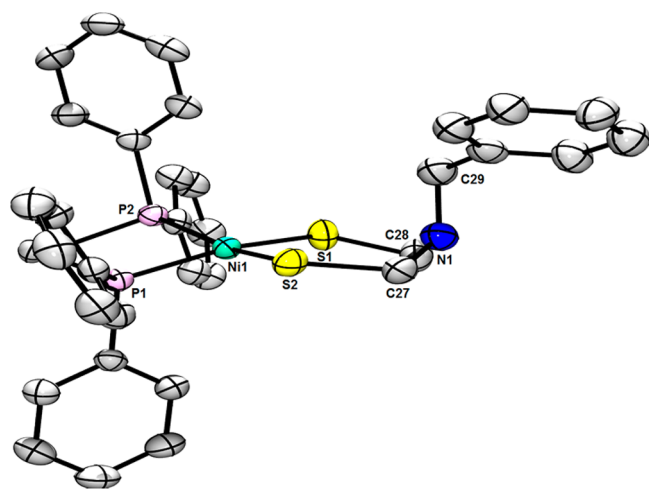


Figure 2. ORTEP of $\text{Ni}[(\text{SCH}_2)_2\text{NBn}](\text{dppe})$ with ellipsoids drawn at the 50% probability level. H atoms and disorder are omitted for clarity. Selected distances (Å): Ni1–S1, 2.1925(10); Ni1–S2, 2.1766(9); Ni1–P1, 2.1840(10); Ni1–P2, 2.1675(9). Selected angles (deg): S1–Ni1–S2, 100.46(3); P1–Ni1–P2, 85.84(3); P1–Ni1–S1, 165.05(3); P2–Ni1–S1, 88.93(3); P1–Ni1–S2, 88.20(3); P2–Ni1–S2, 163.16(3); C27–N1–C28, 112.8(2), C27–N1–C29, 114.6(3); C28–N1–C29, 113.7(2).

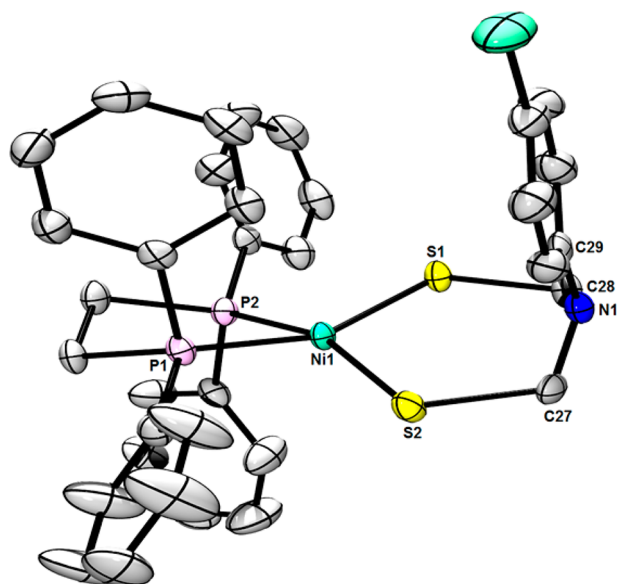


Figure 3. ORTEP of $\text{Ni}[(\text{SCH}_2)_2\text{NC}_6\text{H}_4\text{Cl}](\text{dppe})$ with ellipsoids drawn at the 75% probability level. H atoms and a solvent molecule are omitted for clarity. Selected distances (Å): Ni1–S1, 2.1737(9); Ni1–S2, 2.1792(10); Ni1–P1, 2.1651(10); Ni1–P2, 2.1663(10). Selected angles (deg): S1–Ni1–S2, 104.66(4); P1–Ni1–P2, 85.88(4); P1–Ni1–S1, 156.77(4); P2–Ni1–S1, 87.44(4); P1–Ni1–S2, 89.04(4); P2–Ni1–S2, 158.65(4); C27–N1–C28, 112.7(3), C27–N1–C29, 118.5 (3); C28–N1–C29, 112.00(2).

stereoelectronic effects, this interaction causes the N lone pair to be directed away from the Ni site.

Crystallographic analysis of the complex $\text{Ni}[(\text{SCH}_2)_2\text{NC}_6\text{H}_4\text{Cl}](\text{dppe})$ again reveals a twisted NiS_2P_2 core (Figure 3). The average Ni–S (2.179 Å) and Ni–P bond lengths (2.166 Å) are shortened relative to the benzyl derivative, highlighting a decrease in electron density at the metal center. The distortion of the ligand environments with $\text{R} = 4\text{-ClC}_6\text{H}_4$ is increased relative to the complex with $\text{R} = \text{Bn}$, with a twist of

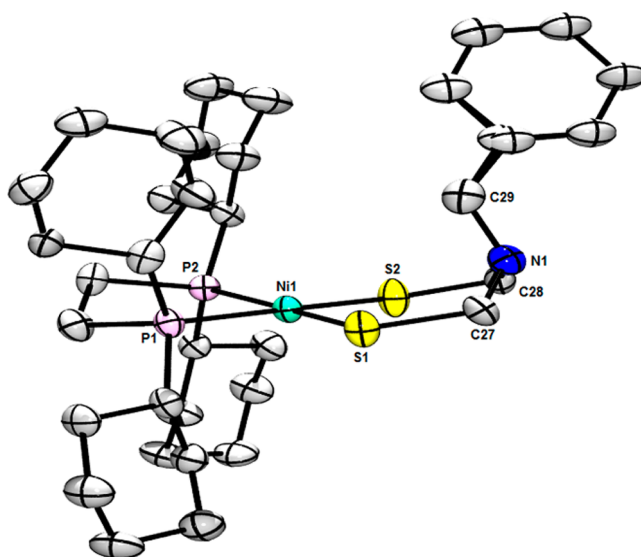


Figure 4. ORTEP of $\text{Ni}[(\text{SCH}_2)_2\text{NBn}](\text{dcpe})\cdot\text{CH}_2\text{Cl}_2$, showing one of the crystallographically independent complexes with ellipsoids drawn at the 50% probability level. H atoms, solvate, and disorder are omitted for clarity. Selected distances (Å): Ni1–S1, 2.1952(19); Ni1–S2, 2.1841(18); Ni1–P1, 2.1884(18); Ni1–P2, 2.1866(18); Ni2–S3, 2.1860(19); Ni2–S4, 2.176(2); Ni2–P3, 2.1774(19); Ni2–P4, 2.1797(18). Selected angles (deg): S1–Ni1–S2, 100.01(7); P1–Ni1–P2, 88.07(7); P1–Ni1–S1, 85.69(7); P2–Ni1–S1, 173.39(7); P1–Ni1–S2, 173.94(8); P2–Ni1–S2, 86.31(7); C27–N1–C28, 113.5(6), C27–N1–C29, 111.3(6); C28–N1–C29, 115.0(6). S4–Ni2–S3, 100.01(8); P3–Ni2–P4, 88.77(7); P3–Ni2–S3, 85.97(7); P4–Ni2–S3, 170.30(8); S4–Ni2–P3, 170.71(9); S4–Ni2–P4, 86.28(7); C62–N2–C63, 112.5(6); C62–N2–C64, 114.7(6); C63–N2–C64, 114.5(6).

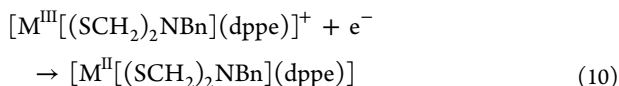
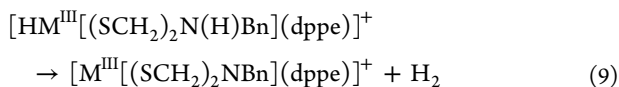
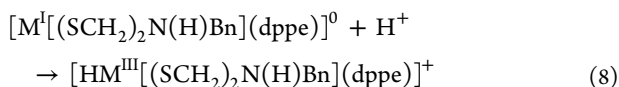
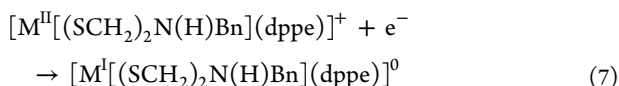
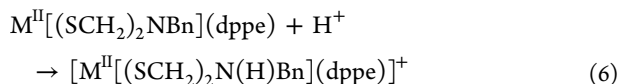
the NiS_2 and NiP_2 planes of 27.6° for the former derivative. The changes in bond lengths and coordination geometry likely reflect the weaker donicity of the $[\text{adt}^{\text{C}_6\text{H}_4\text{Cl}}]^{2-}$ ligand. Containing a more basic diphosphine, $\text{NiCl}_2(\text{dcpe})$ was converted to $\text{Ni}[(\text{SCH}_2)_2\text{NBn}](\text{dcpe})$, albeit in lower yield than in the dppe case. The ^1H and ^{31}P NMR (δ 73.6) and ESI-MS (m/z 676.3) data confirm formation of the target although the sample was not obtained in high purity. Nevertheless, the solid-state structure could be determined by diffraction (Figure 4).

The solid-state structure of $\text{Ni}[(\text{SCH}_2)_2\text{NBn}](\text{dcpe})$ mirrors that of the analogous dppe compound. While the Ni–P and Ni–S bond lengths in the two complexes are virtually identical, the ligand environment in the dcpe complex is less distorted, with the NiS_2 and NiP_2 planes being 2.9° and 10.5° apart in the two crystallographically independent complexes. This planarity might result from the greater size and σ -donicity of dcpe versus dppe. The anion in $\text{BnN}(\text{CH}_2\text{SNa})_2$ was also trapped using $\text{PdCl}_2(\text{dppe})$ as the electrophile, affording crystalline $\text{Pd}[(\text{SCH}_2)_2\text{NBn}](\text{dppe})$, whose ^1H NMR spectrum is similar to that for $\text{Ni}[(\text{SCH}_2)_2\text{NBn}](\text{dppe})$.

Protonation of $\text{Ni}[(\text{SCH}_2)_2\text{NBn}](\text{dppe})$. Treatment of $\text{Ni}[(\text{SCH}_2)_2\text{NBn}](\text{dppe})$ with HOTf (1 equiv) in CD_2Cl_2 resulted in protonation, signaled by a change in color from orange to yellow-orange. The ^{31}P NMR singlet only shifted by 3 ppm downfield upon protonation of the complex, but the ^1H NMR spectrum drastically changed (see Supporting Information)—a new singlet was observed at δ 8.84, assigned to NH , and the symmetry of the $\text{Ni}[(\text{SCH}_2)_2\text{NBn}](\text{dppe})$ is lifted.

While the SCH_2N signals appeared as a broad multiplet for the neutral complex, they appear as doublets-of-triplets for the ammonium species. Consistent with a C_s -symmetric cation, the CH_2Ph signal remains a doublet after protonation. The pK_a^{MeCN} of the amine was not determined since protonation labilizes the complex in this solvent. Nonetheless, addition of increasing amounts of BnNH_3^+ ($pK_a^{\text{MeCN}} = 16.76$) or Bu_3NH^+ ($pK_a^{\text{MeCN}} = 18.03$) to $\text{Ni}[(\text{SCH}_2)_2\text{NBn}](\text{dppe})$ shift the ^{31}P NMR signals toward those of the fully protonated species (see Supporting Information). The complex $\text{Ni}[(\text{SCH}_2)_2\text{-NC}_6\text{H}_4\text{Cl}](\text{dppe})$ did not survive protonation.

Electrochemical Behavior. Cyclic voltammograms (CVs) of $\text{Ni}[(\text{SCH}_2)_2\text{NBn}](\text{dppe})$ in CH_2Cl_2 feature irreversible oxidations at 0.11 V and a reduction at -2.02 V versus $\text{Fc}^{0/+}$. The cathodic wave is shifted to -1.55 V upon addition of 1 equiv of $\text{CF}_3\text{CO}_2\text{H}$ in CH_2Cl_2 . The anodic shift is attributed to protonation of the amine and more facile reduction of the cation $[\text{Ni}[(\text{SCH}_2)_2\text{N(H)Bn}](\text{dppe})]^+$ relative to its conjugate base. Anodic shifts of this magnitude are observed for diiron azadithiolate catalysts.^{3,23} In the presence of $\text{CF}_3\text{CO}_2\text{H}$ (1 equiv), no anodic peaks are observed when scanning in the positive direction. However, once $[\text{Ni}[(\text{SCH}_2)_2\text{NBn}](\text{dppe})]^+$ has been reduced, the anodic peak corresponding to $[\text{Ni}[(\text{SCH}_2)_2\text{NBn}](\text{dppe})]^{0/+}$ reappears. These observations are consistent with the series of electron transfer and chemical steps in eqs 6–10.



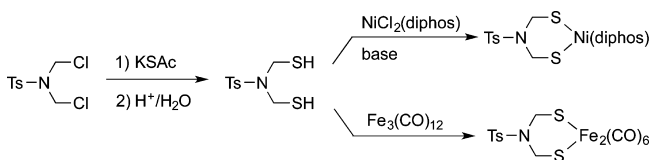
Upon addition of increasing amounts of $\text{CF}_3\text{CO}_2\text{H}$ to $[\text{Ni}[(\text{SCH}_2)_2\text{NBn}](\text{dppe})]^+$, current increases are observed, which are attributed to catalytic reduction of the acid to give H_2 . The dependence of current on $[\text{CF}_3\text{CO}_2\text{H}]$ plateaus at 500 mM of acid, which corresponds to a turnover frequency of 22 s^{-1} according to the usual analysis (see Supporting Information).²⁴

The CV of $\text{Ni}[(\text{SCH}_2)_2\text{NC}_6\text{H}_4\text{Cl}](\text{dppe})$ in CH_2Cl_2 features an irreversible oxidation at 0.22 V and a quasi-reversible reduction at $E_{1/2} = -1.88$ V, both versus $\text{Fc}^{0/+}$. The shifts to more positive potentials for the cathodic and anodic events for the ClC_6H_4 versus Bn derivatives further reflects the influence of the amine substituent on the metal center, despite its remoteness.

TsN(CH₂SH)₂ and Its Fe and Ni Derivatives. The lability of free azadithiols is proposed to be correlated to the basicity of the amine group. This hypothesis suggests that free azadithiols with electron-withdrawing groups on the nitrogen center could

be stable. To address this question, the tosylamide ($\text{MeC}_6\text{H}_4\text{SO}_2\text{NR}_2$, abbreviated TsNR_2) platform was selected since such sulfonamides are known to be nonbasic.²⁵ The targeted $\text{TsN}(\text{CH}_2\text{SH})_2$ was prepared from bis(thioester) $\text{TsN}(\text{CH}_2\text{S}ac)_2$, which in turn was prepared from dichloride $\text{TsN}(\text{CH}_2\text{Cl})_2$ (Scheme 2). Acid-catalyzed hydrolysis of the thioester afforded dithiol $\text{TsN}(\text{CH}_2\text{SH})_2$ as analytically pure white crystals, the ^1H NMR spectrum of which is readily assigned.

Scheme 2. Synthesis of $\text{TsN}(\text{CH}_2\text{SH})_2$ and Its Complexes



The robustness of $\text{TsN}(\text{CH}_2\text{SH})_2$ is further indicated by its efficient conversion to dithiolate complexes. Thus, treatment of the dithiol with $\text{Fe}_3(\text{CO})_{12}$ in hot toluene gave $\text{Fe}_2[(\text{SCH}_2)_2\text{NTs}](\text{CO})_6$, isolated as red crystals. This synthetic method is analogous to the use of alkyl- and arylthiols.²⁶ In addition to its characterization by IR and NMR spectroscopy, $\text{Fe}_2[(\text{SCH}_2)_2\text{NTs}](\text{CO})_6$ was examined by single-crystal X-ray diffraction (Figure 5). Hexacarbonyl $\text{Fe}_2[(\text{SCH}_2)_2\text{NTs}](\text{CO})_6$ is structurally similar to many diiron(I) dithiolates. The Fe centers are within the sum of their covalent radii (2.64 Å for low-spin Fe) with the Fe–Fe distance (2.5145(4) Å) being typical for such compounds, for example, 2.5047(6) Å for $\text{Fe}_2[(\text{SCH}_2)_2\text{NPh}](\text{CO})_6$.¹⁴ Like this

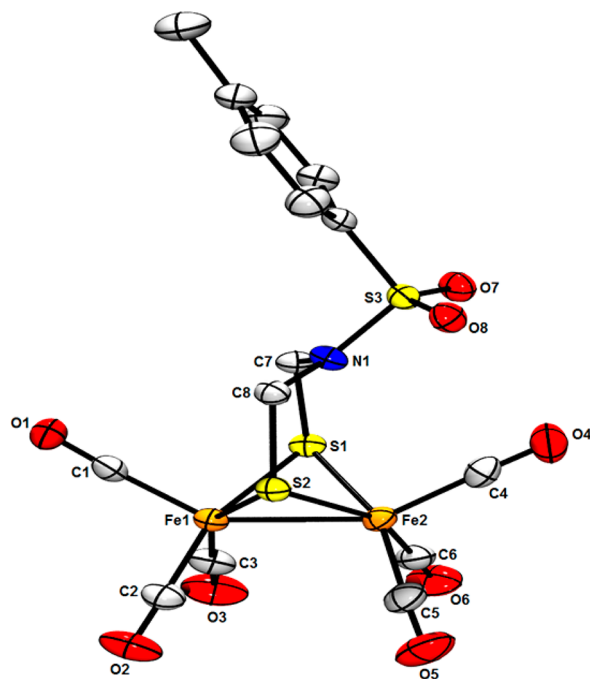


Figure 5. ORTEP of $\text{Fe}_2[(\text{SCH}_2)_2\text{NTs}](\text{CO})_6$ with ellipsoids drawn at the 50% probability level and H atoms omitted for clarity. Selected distances (Å): Fe1–Fe2, 2.5145(4); Fe1–S1, 2.2537(5); Fe2–S2, 2.2547(5); Fe2–S1, 2.2619(5); Fe2–S2, 2.2547(5). Selected angles (deg): Fe1–S1–Fe2, 67.675(15); Fe1–S2–Fe2, 67.718(15); S1–Fe1–S2, 85.735(17); S1–Fe1–Fe2, 56.318(14); C7–N1–S3, 116.45(14); C7–N1–S3, 119.70(11); C8–N1–S3, 120.63(11).

phenyl analogue, the N center in the Ts derivative is roughly trigonal planar, the sum of its bond angles being 357° . Reflecting the nonbasic nature of this tosylamido center, a solution of the diiron complex was found to be unaffected by HBF_4 . The nonbasicity of $\text{Fe}_2[(\text{SCH}_2)_2\text{NTs}](\text{CO})_6$ is in contrast to the easy protonation of other azadithiolato complexes with $\text{R} = \text{alkyl or aryl}$.³

In the presence of base, $\text{TsN}(\text{CH}_2\text{SH})_2$ was also found to react with $\text{NiCl}_2(\text{dppe})$ to give $\text{Ni}[(\text{SCH}_2)_2\text{NTs}](\text{dppe})$, isolated as air-stable red crystals. The structure of this Ni complex was verified by X-ray diffraction (Figure 6).

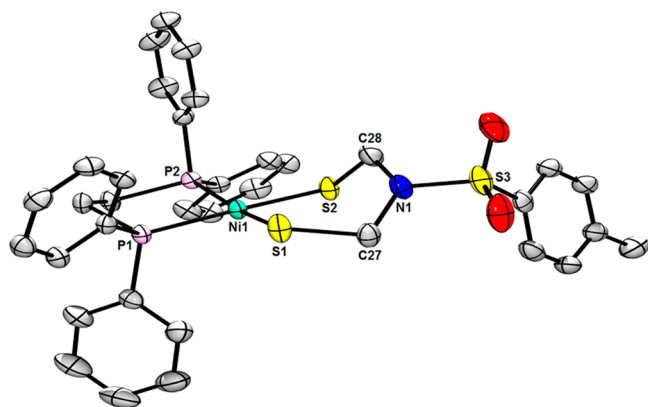


Figure 6. ORTEP of $\text{Ni}[(\text{SCH}_2)_2\text{NTs}](\text{dppe})$ with ellipsoids drawn at the 50% probability level. H atoms and disorder are omitted for clarity. Selected distances (Å): Ni1–S1, 2.1943(5); N1–S2, 2.1963(5); Ni1–P1, 2.1804(5); Ni1–P2, 2.1873(5). Selected angles (deg): S1–Ni1–S2, 94.568(19); P1–Ni1–P2, 87.143(18); P1–Ni1–S1, 90.505(18); P2–Ni1–S1, 168.68(2); P1–Ni1–S2, 173.82(2); P2–Ni1–S2, 88.549(18); C27–N1–C28, 116.95(15), C27–N1–S3, 119.69(13); C28–N1–S3, 117.26(13).

The complex $\text{Ni}[(\text{SCH}_2)_2\text{NTs}](\text{dppe})$ was found to be virtually isostructural to its NBn congener, however, with less distortion of the Ni center (the NiS_2 and NiP_2 interplanar angle being 11.7°). As with the diiron complex, the N atom is approximately planar (angle sum = 354°), but the Ni complex differs in that the sp^2 -hybridization causes puckering of the chelate ring, in contrast to the idealized chair/boat conformation in $\text{Fe}_2[(\text{SCH}_2)_2\text{NTs}](\text{CO})_6$.

CONCLUSIONS

The present work was motivated by the recent confirmation of the azadithiolate ($[\text{adt}^{\text{H}}]^{2-}$) cofactor in the $[\text{FeFe}]$ hydrogenases.¹¹ Our studies were intended to probe the stability of the free azadithiol and its salts. A simplifying aspect of our endeavor was the use of the N-substituted analogues of $[\text{adt}^{\text{H}}]^{2-}$ rather than the secondary amine itself. This compromise was necessary because the precursor $\text{HN}(\text{CH}_2\text{SAC})_2$ is unknown, and a synthesis of this compound could not be devised. The work described here led us to two instructive conclusions.

1. Azadithiolate Salts and Azadithiols Are Labile. The instability is associated with the proximity of the basic nitrogen centers to the thiol groups, this labile motif also being present in the yet-to-be-isolated thioaminals ($\text{R}_2\text{NCH}_2\text{SH}$). In contrast, related compounds are stable when SH is replaced by S-alkyl^{27,28} or when the spacer between the thiol and the amine is extended, as is the case for cysteamine derivatives ($\text{R}_2\text{NCH}_2\text{CH}_2\text{SH}$).²⁷ When the N-substituent is electron-

withdrawing, the corresponding dithiolates appear more stable. This effect is indicated by the improved yields of $\text{Ni}[(\text{SCH}_2)_2\text{NC}_6\text{H}_4\text{Cl}](\text{dppe})$ relative to the N-benzyl derivative. More dramatically, N-substitution with *p*-toluenesulfonyl (Ts) allowed full characterization of the dithiol $\text{TsN}(\text{CH}_2\text{SH})_2$. This dithiol was shown to react efficiently with iron carbonyls to give the corresponding azadithiolatodiiron(I) complex. In this complex, however, the nitrogen center is insufficiently basic to sustain protonation. In terms of their ease of synthesis and low basicity, the $[\text{adt}^{\text{Ts}}]^{2-}$ derivatives resemble analogous N-acetylated ligands $[\text{adt}^{\text{Ac}}]^{2-}$.²⁹

2. Azadithiolate is Stabilized by Coordination, Even to One Metal. Although hundreds of $[\text{adt}^{\text{R}}]^{2-}$ complexes have been reported, few are *not* components of a diiron complex. In this paper, the N-substituted $[\text{adt}^{\text{R}}]^{2-}$ ligands were stabilized through formation of complexes of the familiar $\text{Ni}(\text{dithiolate})\text{-(dppe)}$ motif.³⁰ Aside from the nickel complexes reported in this paper, the titanocene derivatives $(\text{C}_5\text{H}_4\text{R})_2\text{Ti}(\text{adt}^{\text{R}})$ (prepared from $(\text{C}_5\text{H}_4\text{R}')_2\text{Ti}(\text{SH})_2$ and $(\text{CH}_2\text{NR})_3$; $\text{R}' = \text{H, Me}$; $\text{R} = \text{Ph, Me}$) feature nonbridging $[\text{adt}^{\text{R}}]^{2-}$ complexes.¹⁵

Finally, these results have some bearing on the biosynthesis of $[\text{FeFe}]$ hydrogenase. Containing three unusual cofactors, CO, CN^- , and $[\text{adt}^{\text{H}}]^{2-}$, as well as the attached 4Fe–4S cluster, the active site is assembled following a multistep maturation pathway.^{10,31} The source of CO and CN^- has been elucidated, but the origin of $[\text{adt}^{\text{H}}]^{2-}$ remains unsolved. As demonstrated here, the cofactor in its various protonated forms $[\text{H}_n\text{adt}^{\text{H}}]^{(2-n)-}$ is expected to be too unstable to persist in the absence of metal ions. Indeed, the biochemical evidence³² and some literature precedents³³ suggest that the azadithiolate is biosynthesized on an Fe-containing scaffold.

EXPERIMENTAL SECTION

General Considerations. Unless otherwise stated, reactions were conducted using standard Schlenk techniques, and all reagents were purchased from Sigma-Aldrich or Fisher. Unless otherwise noted, all solvents were HPLC grade and purified using an alumina filtration system (Glass Contour, Irvine, CA). ESI-MS data were acquired using a Waters Micromass Quattro II or ZMD spectrometer with analytes in dilute CH_2Cl_2 solution. Analytical data were acquired using an Exeter Analytical CE-440 elemental analyzer. NMR data were acquired using Varian U400, U500, and VXR500 spectrometers. Chemical shifts (in parts per million) were referenced to residual solvent peaks (for ^1H , ^{13}C) or external 85% H_3PO_4 (for ^{31}P). Solution IR spectra were recorded on a PerkinElmer Spectrum 100 FTIR spectrometer. Crystallographic data were collected using a Siemens SMART diffractometer equipped with a Mo $K\alpha$ source ($\lambda = 0.71073 \text{ Å}$) and an Apex II detector.

BnN(CH₂SAC)₂. In a modification of the method of Izawa,²⁰ a solution of benzylamine (10.72 g, 100 mmol) in 100 mL of 95% EtOH was treated with formaldehyde (37% in $\text{MeOH}/\text{H}_2\text{O}$, 24 mL). The mixture was heated at 60°C for 30 min and then treated with AcSH (14.1 mL, 200 mmol). After 2 h, the reaction mixture was cooled to -17°C , when colorless crystals formed. The crystals were isolated by filtration, washed with cold 95% EtOH, and dried briefly under vacuum. Yield: 22.52 g (79%). ^1H NMR (400 MHz, deuterated dimethyl sulfoxide ($\text{DMSO}-d_6$), 298 K): δ 7.34–7.23 (m, 5H, C_6H_5), 4.51 (s, 4H, $\text{C}(\text{O})\text{CH}_2$), 3.61 (s, 2H, PhCH_2), 2.35 (s, 6H, CH_3). ^{13}C NMR (75 MHz, $\text{DMSO}-d_6$, 298 K): δ 196 ($\text{C}=\text{O}$), 137 ($\text{Ph}-\text{C}1$), 129 ($\text{PhC}2$, $\text{PhC}2'$), 128 ($\text{PhC}2$, $\text{PhC}2'$), 128 ($\text{Ph}-\text{C}1$), 56.4 ($\text{C}(\text{O})-\text{CH}_2$), 53.6 (PhCH_2), 31.5 (CH_3). Anal. Calcd for $\text{C}_{13}\text{H}_{17}\text{NO}_2\text{S}_2$: C, 55.09; H, 6.05; N, 4.94. Found: C, 55.24; H, 6.02; N, 4.98%.

Hydrolysis of BnN(CH₂SAC)₂. A solution of $\text{BnN}(\text{CH}_2\text{SAC})_2$ (0.58 g, 2.00 mmol) in 10 mL of EtOH was treated with a 2 M solution of HCl in Et_2O (4.00 mL, 8.00 mmol) under Ar. After the mixture was stirred for 15 h, the white precipitate was isolated by

filtration in air and washed with 2×5 mL of EtOH, yielding 0.370 g of crude product. ^1H NMR analysis ($1,3,5\text{-C}_6\text{H}_3(\text{OMe})_3$ integration standard) of the precipitate showed 63% $[\text{BnNCH}_2\text{SCH}_2]_2$, indicating a yield of 0.23 g of $[\text{BnNCH}_2\text{SCH}_2]_2$ (theoretical yield: 330 mg). The reaction of $\text{BnN}(\text{CH}_2\text{SAC})_2$ with NaOMe afforded the known compound $\text{BnN}(\text{CH}_2\text{OMe})_2$.³⁴

$[\text{BnNCH}_2\text{SCH}_2]_2$. The following is an adaptation of a method for the α -methylbenzylamine derivative.³⁵ A solution of benzylamine (4.9 g, 0.045 mol) in 90 mL of MeOH was added to cold 37% aqueous formaldehyde (27 mL, 0.352 mol) at 0°C . After it was stirred for 5 min at 0°C , the solution was treated with a solution of $\text{NaSH}\cdot x\text{H}_2\text{O}$ (13.53 g, 0.12 mol) in 115 mL of MeOH. After it was stirred for 5 min at 0°C for 24 h, the cloudy solution was concentrated to half its volume under vacuum causing an oil to precipitate. Approximately 30 mL of the oil was separated from the reaction mixture. The oil was mixed with 30 mL of acetone and diluted with 60 mL of EtOH. The solution was concentrated under vacuum until white crystals formed. The crystals were isolated by filtration and washed with 2×20 mL of EtOH. Yield: (0.560 g, 18%). ^1H NMR (500 MHz, $\text{DMSO-}d_6$) δ 7.24–7.34 (m, $J = 15.8, 7.4$ Hz, 10H), 4.54/4.51/4.38/4.35 (ABq, 8H), 3.87 (s, 4H). These data match those from samples prepared according to literature methods.^{23,24} Anal. Calcd for $\text{C}_{18}\text{H}_{22}\text{N}_2\text{S}_2$: C, 65.41; H, 6.71; N, 8.48. Found: C, 65.18; H, 6.66; N, 8.43%. ESI-MS (m/z): 331 (MH^+).

$\text{Ni}[(\text{SCH}_2)_2\text{NBn}](\text{dppe})$. A slurry was prepared of $\text{BnN}(\text{CH}_2\text{SAC})_2$ (283.4 mg, 1.00 mmol), NaO^tBu (192.2 mg, 2.00 mmol), and $\text{NiCl}_2(\text{dppe})$ (528.0 mg, 1.00 mmol) in THF (45 mL) at -78°C with stirring. After 4 h, the purple-red mixture was allowed to warm to room temperature and filtered, with the filtrate being carefully layered with pentane. Red-orange crystals of the product were carefully isolated using a pipet, the remainder of the material (an orange powder) being recrystallized from CH_2Cl_2 /pentane. The combined crops were washed with pentane (2×10 mL) and dried to afford the title compound as red-orange crystals. Yield: 210 mg (32%). ^1H NMR (500 MHz, CD_2Cl_2 , 298 K): δ 7.89 (m, 8H, H2), 7.53 (m, 4H, H4), 7.49 (m, 8H, H3), 7.33 (d, $^3J_{\text{HH}} = 7.5$ Hz, 2H, H2- CH_2Ph), 7.24 (dd, $^3J_{\text{HH}} = 7.5$ Hz, $^3J_{\text{HH}} = 7.5$ Hz, 2H, H3- CH_2Ph), 7.19 (d, $^3J_{\text{HH}} = 7.5$ Hz, 1H, H4- CH_2Ph), 3.99 (s, 2H, CH_2Ph), 3.90 (d, $^4J_{\text{PH}} = 4.3$ Hz, 4H, SCH_2), 2.18 (d, $^3J_{\text{PH}} = 16.9$ Hz, 4H, PCH_2). $^{31}\text{P}\{^1\text{H}\}$ NMR (202 MHz, CD_2Cl_2 , 298 K): δ 57.3. ESI-MS: m/z 654.1 (MH^+). Red prisms of $\text{Ni}[(\text{SCH}_2)_2\text{NBn}](\text{dppe})$ formed upon slow diffusion of pentane layered onto a concentrated CH_2Cl_2 solution of the title compound at -28°C .

Protonation of $\text{Ni}[(\text{SCH}_2)_2\text{NBn}](\text{dppe})$. A solution of $\text{Ni}[(\text{SCH}_2)_2\text{NBn}](\text{dppe})$ (5.4 mg, 8.25 μmol) in 0.5 mL of CD_2Cl_2 in a J-young tube was treated with HOTf (8.4 μL , 1 M) resulting in a color from orange to yellow-orange. ^1H NMR (500 MHz, CD_2Cl_2): δ 8.84 (br. s, 1H, $\text{N}(\text{H})\text{Bn}$), 7.80–7.36 (m, 20 H, PPh_2), 4.19 (dt, $^3J_{\text{HH}} = 12.4, 4.0$ Hz, 2H, SCH_2N), 3.79 (dt, $^3J_{\text{HH}} = 12.4, 4.2$ Hz, 2H, SCH_2N). (ddt, $^3J_{\text{PH}} = 14.3$ Hz, $^3J_{\text{HH}} = 7.9, 3.7$ Hz, 4H, PCH_2). $^{31}\text{P}\{^1\text{H}\}$ NMR (202 MHz, CD_2Cl_2 , 298 K): δ 61.03.

$\text{Ni}[(\text{SCH}_2)_2\text{NBn}](\text{dcpe})$. This compound was prepared as yellow-orange crystals analogously to $\text{Ni}[(\text{SCH}_2)_2\text{NBn}](\text{dppe})$, using $\text{NiCl}_2(\text{dcpe})$ as the precursor. Yield: 28%. ^1H NMR (500 MHz, CD_2Cl_2 , 298 K): δ 7.42–7.18 (m, 5H, Ph), 3.95 (s, 2H, CH_2Ph), 3.89 (d, $^4J_{\text{PH}} = 3.0$ Hz, 4H, SCH_2), 2.58 (d, $^3J_{\text{PH}} = 12.7$ Hz, 2H, PCH), 2.37 (d, $^3J_{\text{PH}} = 12.7$ Hz, 4H, PCH_2), 2.28 (d, $^3J_{\text{PH}} = 13.8$ Hz, 2H, PCH), 2.20–1.46 (m, 40H, $(\text{CH}_2)_5$). ^{31}P NMR (202 MHz, CD_2Cl_2 , 298 K): δ 73.6. ESI-MS: m/z 676.3 (MH^+). Orange blocks of $\text{Ni}[(\text{SCH}_2)_2\text{NBn}](\text{dcpe})\cdot\text{CH}_2\text{Cl}_2$ formed upon slow diffusion of pentane layered onto a concentrated CH_2Cl_2 solution of the title compound at -28°C .

$\text{Pd}[(\text{SCH}_2)_2\text{NBn}](\text{dppe})$. This compound was prepared as orange crystals analogously to $\text{Ni}[(\text{SCH}_2)_2\text{NBn}](\text{dppe})$, using $\text{PdCl}_2(\text{dppe})$ as the precursor. Yield: 24%. ^1H NMR (500 MHz, CD_2Cl_2 , 298 K): δ 7.82 (m, 8H, H2), 7.52 (m, 4H, H4), 7.48 (m, 8H, H3), 7.35 (d, $^3J_{\text{HH}} = 7.6$ Hz, 2H, H2- CH_2Ph), 7.24 (dd, $^3J_{\text{HH}} = 7.9$ Hz, $^3J_{\text{HH}} = 7.9$ Hz, 2H, H3- CH_2Ph), 7.18 (m, 1H, H4- CH_2Ph), 4.19 (s, 2H, CH_2S), 4.19 (s, 2H, CH_2S), 4.17 (s, 2H, CH_2Ph), 2.41 (s, 2H, PCH_2), 2.37 (s, 2H, PCH_2). $^{31}\text{P}\{^1\text{H}\}$ NMR (202 MHz, CD_2Cl_2 , 298 K): δ 50.3. ESI-MS:

m/z 702.1 (MH^+). Anal. Calcd for $\text{C}_{35}\text{H}_{35}\text{NPd}_2\text{S}_2$: C, 59.87; H, 5.02; N, 1.99. Found: C, 59.55; H, 5.12; N, 1.64%.

$\text{ClC}_6\text{H}_4\text{N}(\text{CH}_2\text{SAC})_2$. A solution of 4-chloroaniline (12.76 g, 100 mmol) in 100 mL of 95% EtOH was treated with formaldehyde (37% in methanol/ H_2O , 24 mL). The mixture was heated at 60°C for 30 min and then treated with AcSH (14.1 mL, 200 mmol). After 2 h, the reaction mixture was poured into ~ 100 mL of ice–water, when yellow crystals formed. The crystals were collected by filtration and washed with 100 mL of cold EtOH. Yield: 24.6 g (81%). ^1H NMR (500 MHz, $\text{DMSO-}d_6$, 298 K): δ 7.29 (d, $^3J_{\text{HH}} = 7.69$ Hz, 2H, C_6H_4), 6.80 (d, $^3J_{\text{HH}} = 7.69$ Hz, 2H, C_6H_4), 5.10 (s, 4H, $\text{C}(\text{O})\text{CH}_2$), 2.35 (s, 6H, CH_3). ^{13}C NMR (75.47 MHz, $\text{DMSO-}d_6$, 298 K): δ 196 ($\text{C}=\text{O}$), 143 (C_6H_4), 129 (C_6H_4), 124 (C_6H_4), 116 (C_6H_4), 52.1 ($\text{C}(\text{O})\text{CH}_2$), 31.2 (CH_3). Anal. Calcd for $\text{C}_{12}\text{H}_{14}\text{ClNO}_2\text{S}_2$: C, 47.44; H, 4.64; N, 4.61. Found: C, 47.13; H, 4.5; N, 4.61%. Also prepared analogously was 4-Me $\text{C}_6\text{H}_4\text{N}(\text{CH}_2\text{SAC})_2$. Anal. Calcd for $\text{C}_{13}\text{H}_{17}\text{NO}_2\text{S}_2$: C, 55.09; H, 6.05; N, 4.94. Found: C, 55.24; H, 6.02; N, 4.98%.

$\text{Ni}[(\text{SCH}_2)_2\text{NC}_6\text{H}_4\text{Cl}](\text{dppe})$. A slurry was prepared of $\text{ClC}_6\text{H}_4\text{N}(\text{CH}_2\text{SAC})_2$ (304.8 mg, 1.00 mmol), NaO^tBu (192.2 mg, 2.00 mmol), and $\text{NiCl}_2(\text{dppe})$ (528.0 mg, 1.00 mmol) in THF (45 mL) at -78°C with stirring. After 4 h, the purple-red mixture was allowed to warm to room temperature, resulting in a red solution and some green solid precipitate. The solids were removed by filtration and carefully layered with pentane, affording red-orange crystals. Yield: 505 mg (75%). ^1H NMR (500 MHz, CD_2Cl_2 , 298 K): δ 7.89 (m, 8H, H2), 7.53 (m, 4H, H4), 7.49 (m, 8H, H3), 7.33 (d, $^3J_{\text{HH}} = 7.5$ Hz, 2H, H2- CH_2Ph), 7.24 (dd, $^3J_{\text{HH}} = 7.5$ Hz, $^3J_{\text{HH}} = 7.5$ Hz, 2H, H3- CH_2Ph), 7.19 (d, $^3J_{\text{HH}} = 7.5$ Hz, 1H, H4- CH_2Ph), 3.99 (s, 2H, CH_2Ph), 3.90 (d, $^4J_{\text{PH}} = 4.3$ Hz, 4H, SCH_2), 2.18 (d, $^3J_{\text{PH}} = 16.9$ Hz, 4H, PCH_2) (NMR analysis of the green solid was the same, except for the presence of THF). $^{31}\text{P}\{^1\text{H}\}$ NMR (202 MHz, CD_2Cl_2 , 298 K): δ 57.3. ESI-MS: m/z 654.1 (MH^+). Red prisms of $\text{Ni}[(\text{SCH}_2)_2\text{NBn}](\text{dppe})$ formed upon slow diffusion of pentane layered onto a concentrated CH_2Cl_2 solution of the title compound at -28°C . Anal. Calcd for $\text{C}_{34}\text{H}_{32}\text{ClNNiP}_2\text{S}_2\cdot\text{CH}_2\text{Cl}_2$: C, 55.33; H, 4.51; N, 1.84. Found: C, 55.72; H, 4.35; N, 2.08%.

$\text{TsN}(\text{CH}_2\text{SAC})_2$. A suspension of KSAC (2.73 g, 23.9 mmol) and $\text{TsN}(\text{CH}_2\text{Cl})_2$ ³⁶ (3.06 g, 11.4 mmol) in THF (60 mL) was stirred for 27 h, after which the reaction mixture was filtered to remove NaCl and the colorless filtrate was evaporated to afford a yellow oily residue. A CH_2Cl_2 extract of the crude product was chromatographed on silica gel eluting with 4:1 hexane/EtOAc. The second band was collected, and the solvent was removed to yield the product $\text{TsN}(\text{CH}_2\text{SAC})_2$ as colorless crystals. Yield: 3.04 g (77%). ^1H NMR (400 MHz, CDCl_3 , 293 K): δ 7.69 (d, 2H, H2), 7.32 (d, 2H, H3), 4.89 (s, 4H, NCH_2S), 2.45 (s, 3H, CH_3), 2.31 (s, 6H, $\text{C}(\text{O})\text{CH}_3$). Anal. Calcd for $\text{C}_{13}\text{H}_{17}\text{NO}_4\text{S}_3$: C, 44.94; H, 4.93; N, 4.03. Found: C, 45.17; H, 4.76; N, 4.32%.

$\text{TsN}(\text{CH}_2\text{SH})_2$. A solution of HCl (12 M aqueous, 4.88 mL, 5.76 mmol) in MeOH (100 mL) was sparged with N_2 and then added to a solution of $\text{TsN}(\text{CH}_2\text{SAC})_2$ (0.993 g, 2.86 mmol) in MeOH (20 mL). The resulting homogeneous solution was stirred for 21 h at 50°C , after which solvent evaporation afforded a white residue. A CH_2Cl_2 extract of this solid was chromatographed (SiO_2 , CH_2Cl_2 eluent). The first band was collected and evaporated to dryness to give the dithiol as a white solid. Yield: 310 mg (41%). ^1H NMR (400 MHz, CDCl_3 , 293 K): δ 7.72 (d, 2H, H2), 7.34 (d, 2H, H3), 4.66 (d, 4H, NCH_2S), 2.44 (s, 3H, CH_3), 1.79 (t, 2H, SH). Anal. Calcd for $\text{C}_9\text{H}_{13}\text{NO}_2\text{S}_3$: C, 41.04; H, 4.97; N, 5.32. Found: C, 41.31; H, 4.99; N, 5.19%. mp $51\text{--}53^\circ\text{C}$.

$\text{Fe}_2[(\text{SCH}_2)_2\text{NTs}](\text{CO})_6$. A solution of $\text{TsN}(\text{CH}_2\text{SH})_2$ (263.4 mg, 1.00 mmol) and $\text{Fe}_3(\text{CO})_{12}$ (514.1 mg, 1.02 mmol) in toluene (30 mL) was stirred at 90°C for 3 h, during which time the solution assumed a red color. The reaction mixture was evaporated to yield 472 mg of brick-red solid, which crystallized from CH_2Cl_2 (5 mL) upon the addition of hexanes followed by cooling. Yield: 189 mg (35%). ^1H NMR (400 MHz, CDCl_3 , 293 K): δ 7.50 (d, 2H), 7.30 (d, 2H), 3.65 (s, 4H), 2.43 (s, 3H). FTIR (CH_2Cl_2): ν_{CO} 2080, 2043, 2005, 1985 cm^{-1} . Anal. Calcd for $\text{C}_{15}\text{H}_{11}\text{Fe}_2\text{NO}_8\text{S}_3$: C, 33.29; H, 2.05; N, 2.59. Found: C, 33.10; H, 1.85; N, 2.63%. Red prisms of $\text{Fe}_2[(\text{SCH}_2)_2\text{NTs}](\text{CO})_6$.

(CO)₆ formed upon slow diffusion of hexane layered onto a concentrated CH₂Cl₂ solution of the title compound.

Ni[(SCH₂)₂NTs](dppe). A solution of TsN(CH₂SH)₂ (1.57 g, 6.98 mmol) in 100 mL of CH₂Cl₂ was added to a slurry of NiCl₂(dppe) (2.63 g, 5.00 mmol) and 150 mL of CH₂Cl₂. A solution of NaOEt (0.68 g, 10.0 mmol) in 45 mL of EtOH was added into the mixture. The mixture darkened in color, the NiCl₂(dppe) dissolved, and NaCl precipitated. After the reaction mixture was stirred for 3 h, solvent was removed under vacuum. The product was extracted into CH₂Cl₂ (90 mL). The extract was concentrated to a volume of 10 mL. Brick-red powder precipitated from the concentrate upon the addition of 90 mL of hexane. Yield: 3.15 g (88%). ¹H NMR (500 MHz, CD₂Cl₂, 293 K): δ 7.74 (dd, 8H, Ph), 7.63 (d, 2H, Ts), 7.52 (t, 4H, Ph), 7.46 (t, 8H, Ph), 7.21 (d, 2H, Ts), 4.21 (d, 4H, NCH₂S), 2.38 (s, 3H, CH₃), 2.19 (d, 4H, PCH₂). ¹³C{¹H} NMR (125 MHz, CD₂Cl₂, 293 K): δ 143.2, 134, 132, 130, 129, 128, 125, 121, 43.7, 27.5, 21.6. ³¹P{¹H} NMR (202 MHz, CD₂Cl₂, 293 K): δ 57.6. Anal. Calcd for C₃₅H₃₃NNiO₂P₂S₃: C, 58.51; H, 4.91; N, 1.95. Found: C, 57.88; H, 4.74; N, 2.06%. Red prisms of Ni[(SCH₂)₂NTs](dppe) formed upon slow diffusion of hexane layered onto a concentrated CH₂Cl₂ solution of the title compound.

■ ASSOCIATED CONTENT

● Supporting Information

NMR, ESI-MS, and IR spectra, crystallographic data and structures in CIFs, CV data, and plot of $i_{\text{pcat}}/i_{\text{p}}$ of [Ni[(SCH₂)₂NHBn](dppe)]⁺ (1 mM) versus [CF₃CO₂H] added, where i_{p} is the current with 1 mM acid. The Supporting Information is available free of charge on the ACS Publications website at DOI: 10.1021/acs.inorgchem.5b00290.

■ AUTHOR INFORMATION

Corresponding Author

*E-mail: rauchfuz@illinois.edu.

Present Address

[†]Department of Chemistry, Indian Institute of Technology Kanpur, Kanpur 208016, India.

Notes

The authors declare no competing financial interest.

■ ACKNOWLEDGMENTS

This project was supported by the National Institutes of Health (No. GM061153). R.A. is grateful for the Rubicon grant from The Netherlands Organisation for Scientific Research (NWO). We thank Drs. A. Fuller and C. Richers for advice and assistance.

■ REFERENCES

- (1) Nicolet, Y.; Lemon, B. J.; Fontecilla-Camps, J. C.; Peters, J. W. *Trends Biochem. Sci.* **2000**, *25*, 138–143.
- (2) Barton, B. E.; Olsen, M. T.; Rauchfuss, T. B. *J. Am. Chem. Soc.* **2008**, *130*, 16834–16835.
- (3) Carroll, M. E.; Barton, B. E.; Rauchfuss, T. B.; Carroll, P. J. *J. Am. Chem. Soc.* **2012**, *134*, 18843–18852.
- (4) Camara, J. M.; Rauchfuss, T. B. *J. Am. Chem. Soc.* **2011**, *133*, 8098–8101. Camara, J. M.; Rauchfuss, T. B. *Nat. Chem.* **2012**, *4*, 26–30.
- (5) Nicolet, Y.; de Lacey, A. L.; Vernede, X.; Fernandez, V. M.; Hatchikian, E. C.; Fontecilla-Camps, J. C. *J. Am. Chem. Soc.* **2001**, *123*, 1596–1601.
- (6) Bullock, R. M.; Appel, A. M.; Helm, M. L. *Chem. Commun.* **2014**, *50*, 3125–3143. DuBois, D. L. *Inorg. Chem.* **2014**, *53*, 3935–3960.
- (7) Shook, R. L.; Borovik, A. S. *Inorg. Chem.* **2010**, *49*, 3646–3660.
- (8) Silakov, A.; Wenk, B.; Reijerse, E.; Lubitz, W. *Phys. Chem. Chem. Phys.* **2009**, *11*, 6592–6599. Lubitz, W.; Ogata, H.; Rüdiger, O.; Reijerse, E. *Chem. Rev.* **2014**, *114*, 4081–4148.
- (9) Stich, T. A.; Myers, W. K.; Britt, R. D. *Acc. Chem. Res.* **2014**, *47*, 2235–2243.
- (10) Myers, W. K.; Stich, T. A.; Suess, D. L. M.; Kuchenreuther, J. M.; Swartz, J. R.; Britt, R. D. *J. Am. Chem. Soc.* **2014**, *136*, 12237–12240.
- (11) (a) Berggren, G.; Adamska, A.; Lambert, C.; Simmons, T. R.; Esselborn, J.; Atta, M.; Gambarelli, S.; Mouesca, J.-M.; Reijerse, E.; Lubitz, W.; Happe, T.; Artero, V.; Fontecave, M. *Nature* **2013**, *499*, 66–69. (b) Esselborn, J.; Lambert, C.; Adamska-Venkatesh, A.; Simmons, T.; Berggren, G.; Noth, J.; Siebel, J.; Hemschmeier, A.; Artero, V.; Reijerse, E.; Fontecave, M.; Lubitz, W.; Happe, T. *Nat. Chem. Biol.* **2013**, *9*, 607–609.
- (12) Siebel, J. F.; Adamska-Venkatesh, A.; Weber, K.; Rumpel, S.; Reijerse, E.; Lubitz, W. *Biochem.* **2015**, *54*, 1474–1483.
- (13) Lawrence, J. D.; Li, H.; Rauchfuss, T. B.; Bénard, M.; Rohmer, M.-M. *Angew. Chem., Int. Ed.* **2001**, *40*, 1768–1771.
- (14) Li, H.; Rauchfuss, T. B. *J. Am. Chem. Soc.* **2002**, *124*, 726–727.
- (15) Angamuthu, R.; Carroll, M. E.; Ramesh, M.; Rauchfuss, T. B. *Eur. J. Inorg. Chem.* **2011**, *2011*, 1029–1032.
- (16) Wang, Z.; Liu, J.-H.; He, C.-J.; Jiang, S.; Åkermark, B.; Sun, L.-C. *J. Organomet. Chem.* **2007**, *692*, 5501–5507.
- (17) Das, P.; Capon, J.-F.; Gloaguen, F.; Pétillon, F. Y.; Schollhammer, P.; Talarmin, J.; Muir, K. W. *Inorg. Chem.* **2004**, *43*, 8203–8205.
- (18) Gao, S.; Fan, J.; Sun, S.; Peng, X.; Zhao, X.; Hou, J. *Dalton Trans.* **2008**, 2128–2135.
- (19) Lysenko, N. M. *Zh. Org. Khim.* **1974**, *10*, 2049.
- (20) Izawa, Y.; Terao, Y.; Suzuki, K. *Tetrahedron: Asymmetry* **1997**, *8*, 2645–2648.
- (21) Lin, T.; Ulloa, O. A.; Rauchfuss, T. B.; Gray, D. L. *Eur. J. Inorg. Chem.* **2014**, *2014*, 4109–4114.
- (22) Zhu, W.; Marr, A. C.; Wang, Q.; Neese, F.; Spencer, D. J. E.; Blake, A. J.; Cooke, P. A.; Wilson, C.; Schröder, M. *Proc. Natl. Acad. Sci. U. S. A.* **2005**, *102*, 18280–18285.
- (23) Bourrez, M.; Steinmetz, R.; Gloaguen, F. *Inorg. Chem.* **2014**, *53*, 10667–10673.
- (24) Frazee, K.; Wilson, A. D.; Appel, A. M.; Rakowski DuBois, M.; DuBois, D. L. *Organometallics* **2007**, *26*, 3918–3924.
- (25) (a) Green, T. W.; Wuts, P. G. M. *Protective Groups in Organic Synthesis*; Wiley-Interscience: New York, 1999. (b) Hartung, R.; Golz, G.; Schlaf, S.; Silvennoinen, G.; Polborn, K.; Mayer, P.; Pfendler, H. R. *Synthesis* **2009**, 495–501.
- (26) Tard, C.; Pickett, C. J. *Chem. Rev.* **2009**, *109*, 2245–2274.
- (27) Böhme, H.; Hartke, K. *Chem. Ber.* **1963**, *96*, 604–606.
- (28) (a) Böhme, H.; Kietz, K.; Leidreiter, K. D. *Arch. Pharm.* **1954**, *287*, 198–209. (b) Wellmar, U. J. *Heterocycl. Chem.* **1998**, *35*, 1531–1532. (c) Miyazawa, S.; Ikeda, K.; Achiwa, K.; Sekiya, M. *Chem. Lett.* **1984**, 785–788. (d) Rakhimova, E. B.; Vasil'yeva, I. V.; Khalilov, L. M.; Ibragimov, A. G.; Dzhemilev, U. M. *Chem. Heterocycl. Compd.* **2012**, *48*, 1050–1057. (e) Murzakova, N. N.; Prokofev, K. I.; Tyumkina, T. V.; Ibragimov, A. G. *Russ. J. Org. Chem.* **2012**, *48*, 588–593.
- (29) (a) Stanley, J. L.; Rauchfuss, T. B.; Wilson, S. R. *Organometallics* **2007**, *26*, 1907–1911. (b) Song, L.-C.; Wang, L.-X.; Yin, B.-S.; Li, Y.-L.; Zhang, X.-G.; Zhang, Y.-W.; Luo, X.; Hu, Q. M. *Eur. J. Inorg. Chem.* **2008**, *2008*, 291–297.
- (30) (a) Rauchfuss, T. B.; Roundhill, D. M. *J. Am. Chem. Soc.* **1975**, *97*, 3386–3392. (b) Kochem, A.; Weyhermüller, T.; Neese, F.; van Gastel, M. *Organometallics* **2015**, *34*, 995–1000. (c) Gan, L.; Groy, T. L.; Tarakeswar, P.; Mazinani, S. K. S.; Shearer, J.; Mujica, V.; Jones, A. K. J. *Am. Chem. Soc.* **2015**, *137*, 1109–1115.
- (31) (a) Swanson, K. D.; Duffus, B. R.; Beard, T. E.; Peters, J. W.; Broderick, J. B. *Eur. J. Inorg. Chem.* **2011**, *2011*, 935–947. (b) Dinis, P.; Suess, D. L. M.; Fox, S. J.; Harmer, J. E.; Driesener, R. C.; De La Paz, L.; Swartz, J. R.; Essex, J. W.; Britt, R. D.; Roach, P. L. *Proc. Nat. Acad. Sci. U.S.A.* **2015**, *00*, 0000.
- (32) Peters, J. W.; Broderick, J. B. *Annu. Rev. Biochem.* **2012**, *81*, 429–450.

- (33) (a) Fugate, C. J.; Stich, T. A.; Kim, E. G.; Myers, W. K.; Britt, R. D.; Jarrett, J. T. *J. Am. Chem. Soc.* **2012**, *134*, 9042–9045. (b) Jarrett, J. T. In *Iron-Sulfur Clusters in Chemistry and Biology*; Rouault, T. A., Ed.; Walter de Gruyter: Berlin, Germany, 2014; pp 107–131.
- (34) Mityuk, A. P.; Denisenko, A. V.; Dacenko, O. P.; Grygorenko, O. O.; Mykhailiuk, P. K.; Volochnyuk, D. M.; Shishkin, O. V.; Tolmachev, A. A. *Synthesis* **2010**, *2010*, 493–497.
- (35) Cadenas-Pliego, G.; Jesús Rosales-Hoz, M. d.; Contreras, R.; Flores-Parra, A. *Tetrahedron: Asym.* **1994**, *5*, 633–640.
- (36) Beermann, C.; Ramloch, H. Ger. Offen. DE1915898, 1970.